Adenosine A$_{2A}$ receptor mediates microglial process retraction

Anna G Orr[1], **Adam L Orr**[2], **Xiao-Jiang Li**[2], **Robert E Gross**[3], and **Stephen F Traynelis**[1]

[1]Department of Pharmacology, Emory University School of Medicine, Atlanta, GA 30322, USA.

[2]Department of Human Genetics, Emory University School of Medicine, Atlanta, GA 30322, USA.

[3]Department of Neurosurgery, Emory University School of Medicine, Atlanta, GA 30322, USA.

Abstract

Cell motility drives many biological processes, including immune responses and embryonic development. In the brain, microglia are immune cells that survey and scavenge brain tissue using elaborate motile processes. Motility of these processes is guided by local release of chemoattractants. However, most microglial processes retract during prolonged brain injury or disease. This hallmark of brain inflammation remains unexplained. Here we identified a molecular pathway in mouse and human microglia that converts ATP-driven process extension into process retraction during inflammation. This chemotactic reversal was driven by upregulation of the A$_{2A}$ adenosine receptor coincident with P2Y$_{12}$ downregulation. Thus, A$_{2A}$ receptor stimulation by adenosine, a breakdown product of extracellular ATP, caused activated microglia to assume their characteristic amoeboid morphology during brain inflammation. Our results indicate that purine nucleotides provide an opportunity for context-dependent shifts in receptor signaling. Thus, we reveal an unexpected chemotactic switch that generates a hallmark feature of CNS inflammation.

Brain inflammation is thought to be driven primarily by microglia, the resident hematopoietic cells of the brain and the first responders to most types of central nervous system (CNS) insults. Disturbance in brain homeostasis triggers a rapid response by microglia, which have been termed the "pathology sensors" of the CNS[1,2]. Under normal conditions *in vivo*, microglia exhibit highly branched and motile cell processes that undergo continuous structural remodeling[3–5]. Within minutes of brain damage, these processes rapidly extend toward newly injured areas in order to shield and/or scavenge the affected site[3,4]. This chemoattractive response toward sites of CNS injury is triggered partly by the

release of adenosine triphosphate (ATP) and/or adenosine diphosphate (ADP) from affected tissue and consequent activation of the purinergic P2Y$_{12}$ receptor on microglia5.

In contrast to their ramified morphology under normal conditions, chronic brain damage and neurodegeneration is typically accompanied by microglia with an amoeboid morphology and highly retracted processes1,2,6,7. While microglial process retraction has been documented for over 80 years8 and serves as a defining feature of brain inflammation, its causes and consequences remain unknown. Notably, P2Y$_{12}$ is rapidly downregulated in activated (ie. proinflammatory) microglia, and this decline in P2Y$_{12}$ expression correlates with retraction of microglial processes and adoption of the amoeboid morphology5. However, the basis for this relationship and the triggers of microglial process retraction have not yet been revealed. It also remains unknown whether activated microglia, without expression of P2Y$_{12}$, exhibit any chemotactic response to ATP and/or ADP released during injury. Given that most neuropathologies are characterized by ongoing neuronal injury in the presence of activated microglia, examination of ATP responses by activated microglia may reveal new information about microglial function during neuroinflammation. Here, we investigated the chemotactic and morphological responses by microglia to ATP under both resting and activated states.

RESULTS

Chemotactic and morphological effects of ATP

We first examined whether untreated and activated microglia migrate differently in the presence of ATP, a known microglial chemoattractant released from injured cells4,5,9,10. To activate microglia, cells cultured within a three-dimensional matrix were pretreated for 24 hours with a pattern-recognition receptor agonist lipopolysaccharide (LPS), which activates toll-like receptor 4 (TLR4) and is known to mimic both pathogenic and non-pathogenic immune responses7 (Fig. 1). We then created an ATP gradient by locally applying ATP onto control or LPS-activated microglia using iontophoresis and assessed chemotaxis toward the point source of ATP by performing time-lapse three-dimensional confocal imaging. As expected, localized ATP exposure triggered asymmetric process extension and migration of untreated microglia toward the iontophoretic pipette tip (Fig. 2a–c). Remarkably, LPS-treated microglia exhibited asymmetric retraction of processes and repulsive migration away from the pipette (Fig. 2d–f and Supplementary Video 1). These results indicate that while ATP acts as an attractant for untreated microglia, it acts as a repellant for LPS-treated microglia.

To better understand the intracellular mechanisms driving these opposing chemotactic responses by microglia, we performed time-lapse three-dimensional imaging during bath application of agonist. This method enabled us to quantify changes in microglial cell structure as well as motile responses by individual cell processes without interference from cell migration, since no agonist gradient exists in the recording chamber under these conditions (Fig. 3a–f and Supplementary Fig. 1). In control microglia, we observed that global ATP exposure triggered a rapid and reversible increase in microglial surface area-to-volume ratio (SA:V, Fig. 3g and Supplementary Video 2), reflecting cell process extension. Moreover, tracking individual cell processes revealed that ATP also significantly increased

the velocity of process movement, which we interpret as increased microglial process motility (Fig. 3h). These four-dimensional analyses in control microglia support previous findings that ATP serves as a chemoattractant for resting cells4,5,9,10.

In addition to LPS, we also examined microglia activated with agonists of other pattern recognition receptors, including lipoteichoic acid (LTA, activator of TLR2) or unmethylated CpG motif-containing oligonucleotides (CpG, activator of TLR9). We also examined microglia activated with tumor necrosis factor-α (TNF-α), a proinflammatory cytokine released during most types of brain injuries11. Instead of process extension, activated microglia exhibited symmetric process retraction upon bath application of ATP. Specifically, ATP triggered a decrease in both SA:V ratio and process velocity, reflecting process withdrawal and slowed motility (Fig. 3g–h and Supplementary Video 3 and 4). This shift in response required a prolonged time period (>12 hours), suggesting that changes in protein expression were necessary (Fig. 3i). Consistent with this, blockade of nuclear factor-κB (NF-κB), a transcription factor involved in microglial activation, during pre-treatment prevented retraction and low motility upon ATP exposure (Fig. 3j–k). Complement 5a (C5a), another chemoattractant for microglia12, continued to elicit process extension in LPS-activated microglia (Fig. 3l), suggesting that the shift to repulsion is specific to purinergic stimulation.

Upregulation of the G_S-coupled A_{2A} receptor

We next addressed the receptor signaling mechanisms driving this effect in activated microglia. It is known that resting microglia are attracted to ATP or acute injury at least partly due to Rac GTPase-driven actin polymerization downstream of the G_i-coupled $P2Y_{12}$ receptor3,4,9,10. However, $P2Y_{12}$ is rapidly downregulated upon microglial activation5,13 (Supplementary Fig. 2), suggesting that a different receptor system may mediate chemotactic injury responses by activated microglia. While the signaling mechanisms driving microglial retraction are unknown, other cell types undergo retraction due to remodeling of the actin cytoskeleton, which often involves $G_{12/13}$-coupled activation of Rho GTPase and Rho kinase (ROCK)14,15. Staining microglial actin cytoskeleton suggested that actin remodeling participates in microglial repulsion (Supplementary Fig. 3a–b). However, inhibition of either Rho GTPase or ROCK did not attenuate microglial repulsion (Fig. 4), indicating that an alternative mechanism may drive this response. Interestingly, G_s-coupled signaling can suppress motility in select cell types16,17. This pathway involves activation of adenylate cyclase, which produces cyclic adenosine monophosphate (cAMP) and thereby activates protein kinase A (PKA). We therefore tested whether ATP regulates microglial motility via G_s-coupled signaling. Indeed, inhibition of $G\alpha_s$ or factors downstream of $G\alpha_s$, including adenylate cyclase or PKA, attenuated ATP-induced retraction and slowed motility in activated microglia (Fig. 4a–e and Supplementary Fig. 3c–d). Conversely, stimulating adenylate cyclase with forskolin induced dose-dependent retraction in both control and activated microglia (Fig. 4f). Moreover, constitutive activation of $G\alpha_s$ with cholera toxin blunted membrane extension in unstimulated cells and induced microglial cell rounding within 24 hours (data not shown). These results indicate that G_s signaling is necessary and sufficient for microglial repulsion.

Together, our data implicate a G_s-coupled receptor in the chemorepulsion of activated microglia by ATP. However, there is no known G_s-coupled mouse P2Y receptor. Therefore, we considered other receptor classes. Upon release in the brain, ATP is rapidly broken down to adenosine by extracellular and membrane-bound nucleotidases, including CD39 and CD73[18]. Thus, we investigated the role of adenosine receptors, two of which (A_{2A} and A_{2B}) are G_s-coupled[19]. Reverse transcription-polymerase chain reaction (RT-PCR) revealed that, while $P2Y_{12}$ is lost, the high-affinity adenosine receptor A_{2A} is selectively upregulated upon microglial activation with toll-like receptor agonists or with TNF-α (Fig. 5a). Indeed, A_{2A} mRNA upregulation has been observed previously in microglia treated with LPS, but not functionally studied[20]. Notably, aggregated amyloid-β (Aβ), a main component of extracellular amyloid plaques in Alzheimer's disease, also triggered microglial A_{2A} upregulation and $P2Y_{12}$ downregulation (Fig. 5a).

In support of a functional role of A_{2A} in repulsion, we found that both NECA, a nonselective adenosine receptor agonist, and CGS-21680, an A_{2A}-selective agonist[18,19], mimicked ATP by triggering retraction in activated microglia, but the agonists had little effect on unstimulated microglia (Fig. 5b and data not shown). Moreover, the A_{2A}-selective antagonist SCH-58261[18,19] attenuated microglial repulsion from ATP (Fig. 5c), further suggesting that A_{2A} mediates repulsion. While ATP does not activate the A_{2A} receptor directly, it is rapidly hydrolyzed into adenosine, which is a potent activator of the A_{2A} receptor (Supplementary Fig. 4)[18]. Reasoning that ATP degradation into adenosine is a necessary step leading to microglial repulsion, we stimulated cells with ATP in the presence of adenosine deaminase (ADA), which converts adenosine into inosine. Consistent with our working hypothesis, ADA inhibited retractile responses (Fig. 5c), demonstrating that ATP-induced microglial repulsion is mediated by the ATP breakdown product adenosine.

Interestingly, A_{2A} receptor upregulation has also been reported in human macrophages and in brain tissue from Alzheimer's disease patients[21,22]. Thus, we investigated whether adult human microglia also upregulate A_{2A} expression upon inflammation-driven activation and consequently display chemotactic reversal in response to ATP. We observed that LPS-activated adult human microglia exhibited marked A_{2A} upregulation along with a loss in $P2Y_{12}$ expression (Fig. 6a). Importantly, while unstimulated human microglia showed migration toward and engulfment of an ATP-filled pipette, LPS-stimulated human microglia exhibited repulsion (Fig. 6b and Supplementary Videos 5 and 6). Thus, a similar chemotactic switch takes place in adult human microglia.

Role of A_{2A} receptor in process retraction and scavenging

We next investigated whether the A_{2A} receptor plays a role in the retracted morphology assumed by activated microglia during neuroinflammation *in vivo*. For this, we utilized a well-established animal model of neuroinflammation involving systemic LPS exposure[7]. Using transgenic *Adora-eGFP* mice that express eGFP under control of the A_{2A} promoter, we first confirmed that A_{2A} receptor upregulation takes place *in vivo* following LPS treatment (Fig. 7a). Next, we utilized transgenic *Cx3Cr1-eGFP* mice that exhibit microglia-specific eGFP labeling[3–5]. We note that although eGFP is localized exclusively in microglial cells among CNS-resident cellular elements, the fluorescent reporter does not

differentiate between resident microglia and infiltrating mononuclear phagocytes, which may exhibit microglial morphology. Upon LPS exposure, these animals displayed characteristic retracted microglia throughout the brain, a hallmark of activated microglia and induction of CNS inflammation (Supplementary Fig. 5). In these LPS-treated animals, we observed that intracortical injection of the A_{2A}-specific antagonist SCH-58261 resulted in microglial process re-extension within 30 minutes, an effect not seen in animals injected with vehicle alone (Fig. 7b and Supplementary Fig. 5). These observations are consistent with our *in vitro* data and suggest that activated microglia may assume an amoeboid phenotype *in vivo* due to A_{2A} receptor stimulation by purine nucleotides released in the brain.

Previous studies have shown that acute injury results in the release of ATP and other nucleotides from damaged cells, which triggers chemoattraction of microglial processes toward sites of injury[4,5]. We therefore asked whether acute tissue damage can repel processes of activated microglia. To address this, we performed time-lapse imaging on eGFP[+] microglia co-cultured with wild-type astrocytes that received focal injury with a pipette tip. We observed that acute damage triggers adjacent microglia to extend processes toward injury (n = 3, Supplementary Video 7). However, following co-culture exposure to LPS, damage triggers microglial retraction from the injury site (n = 6, Supplementary Video 8), suggesting that the chemotactic response of microglial processes to acute tissue damage may be reversed during inflammation. We also examined whether A_{2A}-driven process retraction may influence the rate of phagocytosis by cultured microglia. Indeed, we observed a decrease in particle uptake by LPS-treated microglia in the presence of A_{2A} agonists, including CGS-21680, adenosine, or ATP (Fig. 8), suggesting that A_{2A} stimulation may modulate substrate engulfment by activated microglia.

DISCUSSION

Activated microglia are known to retract into an amoeboid shape during neurological disease or trauma. The cause and significance of this phenomenon have remained unknown. Here, we report that the microglial chemotactic response to ATP is reversed upon microglial activation. This reversal, a switch from process attraction to repulsion, is driven by upregulation of the G_s-coupled A_{2A} receptor coincident with downregulation of the G_i-coupled $P2Y_{12}$ receptor (see schematic in Supplementary Fig. 6). We further propose that degradation of extracellular ATP to adenosine by ectonucleotidases, such as CD39 and CD73, which are thought to be expressed by microglia[23–26], leads to activation of the adenosine A_{2A} receptor and consequent process retraction by activated microglia. Given that extracellular ATP and its metabolite adenosine are ubiquitous in the brain[27–31], our results suggest that activated microglia may assume their characteristic amoeboid morphology due to A_{2A}-driven process repulsion from endogenously produced adenosine.

To our knowledge, this is the first extracellular signaling factor that acts to repel microglial processes, an aspect of neuroimmune responses that requires further study. Moreover, our findings of A_{2A} agonist effects on microglial phagocytosis suggest that this receptor may impact microglial function beyond process retraction. Thus, additional research into the effects of A_{2A} receptor stimulation on activated microglia is needed to fully elucidate the

roles that this receptor plays in microglial activity. We also conclude that G_s-coupled intracellular signaling may be an important regulator of microglial function, as suggested previously[32–34]. Further investigation into the effects of G_s-coupled signaling in microglia may help to address long-standing and fundamental questions regarding the nature of microglial activation and may reveal novel therapeutic strategies for CNS diseases.

Interestingly, A_{2A} gene ablation and A_{2A} receptor antagonists, including caffeine, are known to modulate brain injury in animal models of CNS trauma and neurodegeneration[35–37]. However, while neuronal and astrocytic A_{2A} receptors are thought to be involved in brain injury, the effects of microglial A_{2A} receptor upregulation during inflammation require further investigation. While we and others[20] have shown that microglial A_{2A} expression is only evident following proinflammatory activation, some studies have suggested that A_{2A} may also be expressed by cultured microglia prior to activation[38–40]. However, we have not been able to detect microglial A_{2A} expression in normal *Adora-eGFP* mice or in untreated cultured mouse or human microglia using RT-PCR or time-lapse three-dimensional imaging with A_{2A} agonists. Thus, the state of microglial activation and the specific pattern of purinergic receptor expression may vary under different conditions.

In summary, our results suggest that A_{2A}-dependent repulsion is a major driving force for microglial deramification, a hallmark of neuroinflammation. Our data also reveal a flexible duality in microglial cell motility. We show that microglial motility can switch between chemoattraction and repulsion based on changes in cell surface receptor signaling. These results demonstrate a previously unrecognized adaptive feature of microglial motility that allows ATP to induce an opposite chemotactic response during inflammation.

METHODS

Cell cultures

All procedures were approved by the Institutional Animal Care and Use Committee or the Emory Institutional Review Board. Mice expressing enhanced green fluorescent protein (eGFP) driven by an actin promoter (a gift from M. Okabe, Osaka University, Japan) were used to culture microglia. Cortical tissue from postnatal day 2–3 *actin-eGFP* or wild-type C57Bl/6 mice (The Jackson Laboratory) was dissociated and plated with serum-supplemented DMEM (Gibco #11960) containing (mM): 25 glucose, 2 glutamine, and 1 Na pyruvate. After 2–3 weeks, floating microglia were isolated and plated onto Matrigel matrix-coated coverslips (BD Biosciences, thickness ∼ 0.2 mm). Microglia adhered overnight and were confirmed 95% pure based on IB4 staining (data not shown). For astrocyte-microglia co-cultures, eGFP microglia were applied onto 50% confluent wild-type astrocytes and allowed to adhere overnight. Human microglia were cultured as previously described[41]. Adult human microglial cells were obtained from two Emory University Hospital patients (ages 30–45) undergoing hippocampectomy due to seizures or resection due to a subarachnoid tumor. Human microglia were allowed to adhere for 5–7 days prior to imaging.

Reagents

Adenosine 5′-triphosphate (ATP), adenosine 5′-diphosphate (ADP), adenosine 5′-monophosphate (AMP), 5′-(N-ethylcarboxamido)adenosine (NECA), adenosine, A2a agonist CGS-21680, A2a antagonist SCH-58261, lipopolysaccharide (LPS), lipoteichoic acid from *Staphylococcus aureus* (LTA), Gαs inhibitor NF449, and the protein kinase A (PKA) inhibitor H89 were all purchased from Sigma. Nuclear factor-κB (NF-κB) inhibitors 6-Amino-4-(4-phenoxyphenylethylamino)quinazoline (QNZ) and SN50, forskolin (FSK), adenylate cyclase inhibitor 2′,5′-dideoxyadenosine (ddAdo), Gαs activator cholera toxin (*Vibrio cholerae*, CLX), Rho GTPase inhibitor exoenzyme C3 (*Clostridium botulinum)*, Rho kinase (ROCK) inhibitor Y27632, and adenosine deaminase (ADA) were all purchased from Calbiochem. We also utilized recombinant mouse complement component C5a, recombinant mouse TNF-α (R&D Systems), and unmethylated CpG motif-containing oligonucleotides (CpG, InvivoGen). Isolectin GS-IB$_4$ (IB$_4$) from *Griffonia simplicifolia* and human β-amyloid 1–42 (aggregated according to manufacturer instructions) was obtained from Invitrogen.

Four-dimensional confocal imaging

Cells were continuously perfused with imaging buffer (mM): 10 HEPES, 150 NaCl, 3 KCl, 22 Sucrose, 10 Glucose, 1 MgCl2, and 2 CaCl2, pH 7.4. The buffer was maintained at 32–33.5°C using TC-344B temperature controller (Warner Instruments). After establishing upper and lower z-axis limits, time-lapse confocal image stacks of eGFP microglia were acquired every 15–20 seconds. Each image stack spanned the entire z-plane of microglia at 0.5–2 μm steps (25–30 images per stack). Image stacks were acquired using IPlab software (BD Biosciences), Olympus IX51 microscope with DSU confocal unit, a MFC-2000 z-motor (ASI) and a Uniblitz shutter (Vincent Associates). Image stacks were collected continuously during 5 min periods of buffer perfusion, agonist perfusion, and washout with an ORCA-ER cooled CCD camera (Hamamatsu).

Image processing and analysis

Following acquisition, images were compiled and transformed into four-dimensional renderings of microglia throughout the course of a perfusion using Imaris 4.2 (Bitplane). After background noise subtraction with a 10 μm-width Gaussian filter, image stacks were reconstructed into three-dimensional surfaces at each time-point based on calibrated voxel sizes (x/y: 0.105 μm^2, z: 0.5–2 μm), a signal intensity threshold, and a 0.2 μm-width Gaussian filter. All time-lapse surfaces were then split into objects to enable measurements of cell volume and surface area through time. Cell surface area-to-volume ratio (SA:V) at each time-point was then calculated to assess changes in cell structure.

Microglial cell process motility was assessed by comparing average speed of tracked regions of interest (ROIs) within cell processes during periods of buffer and agonist perfusion. ROIs, or discrete spherical volumes of fluorescence, were analyzed based on pre-defined criteria, such as minimum diameter, maximum travel distance between consecutive image stacks, and the type of tracking algorithm utilized. To assign ROIs to cell processes and enable tracking, we first optimized these criteria. While varying these parameter values, we compared sensitivity and reliability of the tracking analysis to agonist-induced changes in

track speed, number of tracks, and track length (Supplementary Fig. 1, and data not shown). Additionally, we minimized changes in the number of unassigned ROIs (i.e. regions not designated by the algorithm to any track). As determined empirically, the parameter values we held constant for all analyses of process motility were 2 μm minimum diameter, 3 μm maximum travel distance and GapClose Autoregressive tracking algorithm, a function which matches predicted ROI positions with actual ROI positions within image data and thereby models continuous motion. Tracks created within the cell body were omitted from analyses. Baseline process ramification of control group was lower than that of CpG- and TNF-α-treated groups ($p < 0.01$), but not different from LPS- and LTA-treated groups. Baseline process motility of control group was lower than that of CpG- and LPS-treated groups ($p < 0.01$), but not different from LTA- and TNF-α-treated groups.

Iontophoresis

A glass micropipette (inner diameter: 1.15 ± 0.05 mm, outer diameter: 1.65 ± 0.05 mm, glass type 8250, Garner Glass Co.) was pulled to a ~1.4 MΩ tip with a Narishige pipette puller, filled with agonist diluted in imaging buffer, and attached to a micromanipulator and a current generator (Model 6400, Dagan). The positive holding current value (+80 nA) was determined empirically by observing microglial morphological responses (occurrence of membrane ruffling) while in close proximity to an ATP-containing micropipette with different holding currents. Agonist application was performed by ejecting a −200nA current. In order to analyze cell chemotaxis in response to iontophoretic agonist application, cell body was tracked by setting ROI diameter to the size of the nucleus.

Actin filament staining

Cultured wild-type microglia were treated with agonists, fixed and stained with 1:100 Alexa Fluor-488 phalloidin (Invitrogen) and 1:100 IB4 to identify microglia.

In vivo injections and immunohistochemistry

Transgenic mice that encode eGFP in place of exon 2 within the *Cx3cr1* gene were obtained from the Jackson Laboratory. Animals (1–3 month old) received a single intraperitoneal injection of either sterile PBS or LPS (2 mg/kg, 100 μl total volume). After 48 hours, mice were anesthetized with Avertin and placed into a stereotaxic apparatus for an intracortical injection of vehicle (50% DMSO in PBS, 2 μl) or the A2A antagonist SCH-58261 (1 mM in 2 μl) at 400 nl per minute at 1.0 mm caudal, 2.0 mm lateral, and 1.0 mm ventral from bregma. The needle was left in place for 5 minutes. After another 25 minutes, brain tissue was removed and drop-fixed overnight in 4% paraformaldehyde with 0.1% glutaraldehyde and cryopreserved in sucrose. 40 μm-thick sections were washed in PBS and placed on slides for microscopy. *Adora-eGFP* BAC transgenic mice were obtained from the Mutant Mouse Regional Resource Centers and received an intraperitoneal injection of either sterile PBS or LPS (2 mg/kg, 100 μl total volume). After 48–72 hours, tissue was processed and immunostained using anti-GFP antibody (1:1000, Invitrogen).

RT-PCR

Total RNA was derived from homogenized primary mouse microglia according to manufacturer instructions using Purelink Micro-to-Midi total RNA purification system (Invitrogen). RNA (50 ng) was then reverse transcribed and amplified using SuperScript III One-Step RT-PCR System with Platinum *Taq* (Invitrogen) and specific primers, as detailed previously[5,42–50]. cDNA synthesis was carried out at 50°C for 30 min, followed by pre-denaturation at 94°C for 2 min, 30–40 cycles of denaturation at 94°C for 15 sec, annealing at 55°C for 30 sec (except for P2Y4: 51°C; hP1 receptors: 58°C; activation markers: 60°C), and finally elongation at 70°C for 1 min. To check for DNA contamination, reverse transcriptase was omitted from some reaction mixtures. For primer pairs that did not produce visible bands using isolated RNA, 2 ng cDNA encoding each receptor was used to run control reactions. Plasmids for mouse adenosine receptors and mP2Y2 were from Open Biosystems, while mP2Y4 and mP2Y6 were a gift from W. O'Neal at the University of North Carolina, Chapel Hill.

Uptake assay

Microglial phagocytosis was analyzed using the Vybrant phagocytosis assay kit (Invitrogen) according to manufacturer instructions. Briefly, primary mouse microglia were isolated, allowed to adhere overnight onto 0.05 mg/ml poly-D-lysine-coated 96-well plates, and treated with LPS (100 ng/ml) at 37°C for 24 hours. After pre-exposure to ATP (50 μM), CGS-21680 (50 μM), or adenosine (50 μM) for 20 min, fluorescein-labeled *Escherichia coli* bioparticles were applied for 2 hours along with agonists. Cells were examined using the FlexStation II microplate reader (Molecular Devices) at 480 nm excitation and 520 nm emission. Results were normalized to empty wells and DMEM-treated cells.

cAMP assay

Agonist-induced release of cAMP was measured using the CatchPoint Cyclic-AMP Fluorescence Assay kit (Molecular Devices) with some modification to manufacturer instructions. Briefly, HEK 293 cells were plated with DMEM-Glutamax supplemented with 10% fetal bovine serum, 10 U/ml penicillin, and 10 μg/ml streptomycin, and transfected with cDNA encoding the mouse A_{2A} receptor (Open Biosystems) at 3:1 ratio using FuGene 6 (Roche). HEK cells were then incubated in 0.75 mM 3-isobutyl-1-methylxanthine (IBMX, Sigma) for 10 minutes to inhibit phosphodiesterase activity. Indicated agonists or 30 μM forskolin (activator of adenylate cyclase) were then added for 15 minutes at 37°C. Fluorescence intensity in each well was detected using the FlexStation II plate reader (Molecular Devices) using 530 nm excitation and 590 nm emission.

Statistics

All statistical tests were performed on raw data except for the phagocytosis analysis. Average cell ramification, process track speed, and migration during baseline were compared to periods of agonist exposure using a paired Student's t-test. Data were normally distributed and had equal variances, as verified using Bartlett's test. Analyses of different pre-treatment conditions or inhibitor effects on agonist responses in the confocal imaging experiments were performed using repeated-measures two-way ANOVA. cAMP release was

analyzed with one-way ANOVA and Dunn's multiple comparisons post-test. Phagocytosis analysis was performed with the Kruskal-Wallis test and Dunn's multiple comparisons post-test.

Supplementary Material

Refer to Web version on PubMed Central for supplementary material.

ACKNOWLEDGEMENTS

REFERENCES

1. Hanisch UK, Kettenmann H. Microglia: active sensor and versatile effector cells in the normal and pathologic brain. Nat Neurosci. 2007; 10:1387–1394. [PubMed: 17965659]

2. Kreutzberg GW. Microglia: a sensor for pathological events in the CNS. Trends Neurosci. 1996; 19:312–318. [PubMed: 8843599]

3. Nimmerjahn A, Kirchhoff F, Helmchen F. Resting microglial cells are highly dynamic surveillants of brain parenchyma *in vivo*. Science. 2005; 308:1314–1318. [PubMed: 15831717]

4. Davalos D, et al. ATP mediates rapid microglial response to local brain injury in vivo. Nat Neurosci. 2005; 8:752–758. [PubMed: 15895084]

5. Haynes SE, et al. The P2Y12 receptor regulates microglial activation by extracellular nucleotides. Nat Neurosci. 2006; 9:1512–1519. [PubMed: 17115040]

6. Stence N, Waite M, Dailey ME. Dynamics of microglial activation: a confocal time-lapse analysis in hippocampal slices. Glia. 2001; 33:256–266. [PubMed: 11241743]

7. Block ML, Zecca L, Hong JS. Microglia-mediated neurotoxicity: uncovering the molecular mechanisms. Nat Rev Neurosci. 2007; 8:57–69. [PubMed: 17180163]

8. Jakob, A. Handbuch der Psychiatrie 1. Aschaffenburg, G., editor. Deuticke; 1927. p. 268

9. Nasu-Tada K, Koizumi S, Inoue K. Involvement of β1 integrin in microglial chemotaxis and proliferation on fibronectin: different regulations by ADP through PKA. Glia. 2005; 52:98–107. [PubMed: 15920726]

10. Honda S, et al. Extracellular ATP or ADP induce chemotaxis of cultured microglia through Gi/o-coupled P2Y receptors. J Neurosci. 2001; 21:1975. [PubMed: 11245682]

11. Wang CX, Shuaib A. Involvement of inflammatory cytokines in central nervous system injury. Prog Neurobiol. 2002; 67:161–172. [PubMed: 12126659]

12. Nolte C, Moller T, Walter T, Kettenmann H. Complement 5a controls motility of murine microglial cells in vitro via activation of an inhibitory G-protein and the rearrangement of the actin cytoskeleton. Neuroscience. 1996; 73:1091–1107. [PubMed: 8809827]

13. Moller T, Kann O, Verkhratsky A, Kettenmann H. Activation of mouse microglial cells affects P2 receptor signaling. Brain Res. 2000; 853:49–59. [PubMed: 10627307]

14. Burridge K, Wennerberg K. Rho and Rac take center stage. Cell. 2004; 116:167–179. [PubMed: 14744429]

15. Mitchison TJ, Cramer LP. Actin-based cell motility and cell locomotion. Cell. 1996; 84:371–379. [PubMed: 8608590]

16. Nagasawa S, Takuwa N, Sugimoto N, Mabuchi H, Takuwa Y. Inhibition of Rac activation as a mechanism for regulation of actin cytoskeletal reorganization and cell motility by cAMP. Biochem J. 2005; 385:737–744. [PubMed: 15377280]

17. Hashmi AZ, et al. Adenosine inhibits cytosolic calcium signals and chemotaxis in hepatic stellate cells. Am J Physiol Gastrointest Liver Physiol. 2007; 292:G395–G401. [PubMed: 17053161]

18. Fredholm BB, IJzerman AP, Jacobson KA, Klotz KN, Linden J. International Union of Pharmacology. XXV. Nomenclature and classification of adenosine receptors. J. Pharmacol Rev. 2001; 53:527–552.

19. Ongini E, Fredholm BB. Pharmacology of adenosine A_{2A} receptors. Trends Pharmacol Sci. 1996; 17:364–372. [PubMed: 8979771]

20. Wittendorp MC, Boddeke HWGM, Biber K. Adenosine A3 receptor-induced CCL2 synthesis in cultured mouse astrocytes. Glia. 2004; 46:410–418. [PubMed: 15095371]

21. Angulo E, et al. A1 adenosine receptors accumulate in neurodegenerative structures in Alzheimer's disease and mediate both amyloid precursor protein processing and tau phosphorylation and translocation. Brain Pathol. 2003; 13:440–451. [PubMed: 14655750]

22. Murphree LJ, Sullivan GW, Marshall MA, Linden J. Lipopolysaccharide rapidly modifies adenosine receptor transcripts in murine and human macrophages: role of NF-kappaB in A(2A) adenosine receptor induction. Biochem J. 2005; 391:575–580. [PubMed: 16022683]

23. Braun N, Lenz C, Gillardon F, Zimmermann M, Zimmermann H. Focal cerebral ischemia enhances glial expression of ecto-5'-nucleotidase. Brain Res. 1997; 766:213–226. [PubMed: 9359605]

24. Braun N, et al. Assignment of ecto-nucleoside triphosphate diphosphohydrolase-1/cd39 expression to microglia and vasculature of the brain. Eur J Neurosci. 2000; 12:4357–4366. [PubMed: 11122346]

25. Schoen SW, Graeber MB, Kreutzberg GW. 5'-Nucleotidase immunoreactivity of perineural microglia responding to rat facial nerve axotomy. Glia. 2004; 6:314–317. [PubMed: 1464463]

26. Färber K, et al. The ectonucleotidase cd39/ENTPDase1 modulates purinergic-mediated microglial migration. Glia. 2008; 56:331–341. [PubMed: 18098126]

27. Rodriguez-Nunez A, et al. Concentrations of nucleotides, nucleosides, purine bases, oxypurines, uric acid, and neuron-specific enolase in the cerebrospinal fluid of children with sepsis. J Child Neurol. 2001; 16:704–706. [PubMed: 11575617]

28. Guthrie PB, et al. ATP released from astrocytes mediates glial calcium waves. J Neurosci. 1999; 19:520–528. [PubMed: 9880572]

29. Koizumi S, Fujishita K, Tsuda M, Shigemoto-Mogami Y, Inoue K. Dynamic inhibition of excitatory synaptic transmission by astrocyte-derived ATP in hippocampal cultures. Proc Natl Acad Sci USA. 2003; 100:11023–11028. [PubMed: 12958212]

30. Verderio C, Matteoli M. ATP mediates calcium signaling between astrocytes and microglial cells: modulation by IFN-gamma. J Immunol. 2001; 166:6383–6891. [PubMed: 11342663]

31. Pedata F, Corsi C, Melani A, Bordoni F, Latini S. Adenosine extracellular brain concentrations and role of A2A receptors in ischemia. Ann N Y Acad Sci. 2001; 939:74–84. [PubMed: 11462806]

32. Tomozawa Y, Yabuuchi K, Inoue T, Satoh M. Participation of cAMP and cAMP-dependent protein kinase in beta-adrenoceptor-mediated interleukin-1 beta mRNA induction in cultured microglia. Neurosci Res. 1995; 22:399–409. [PubMed: 7478305]

33. Zhang B, et al. Suppressive effects of phosphodiesterase type IV inhibitors on rat cultured microglial cells: comparison with other types of cAMP-elevating agents. Neuropharmacol. 2002; 42:262–269.

34. Min KJ, Yang MS, Jou I, Joe EH. Protein kinase A mediates microglial activation induced by plasminogen and gangliosides. Exp Mol Med. 2004; 36:461–467. [PubMed: 15557818]

35. Schwarzschild MA, Agnati L, Fuxe K, Chen JF, Morelli M. Targeting adenosine A2A receptors in Parkinson's disease. Trends Neurosci. 2006; 11:647–654. [PubMed: 17030429]

36. Xu K, Bastia E, Schwarzschild M. Therapeutic potential of adenosine A(2A) receptor antagonism in Parkinson's disease. Pharmacol Ther. 2004; 105:267–310. [PubMed: 15737407]

37. Popoli P, et al. Functions, dysfunctions and possible therapeutic relevance of adenosine A_{2A} receptors in Huntington's disease. Prog Neurobiol. 2007; 81:331–348. [PubMed: 17303312]

38. Fiebich, et al. Cyclooxygenase-2 expression in rat microglia is induced by adenosine A2a-receptors. Glia. 1996; 18:152–160. [PubMed: 8913778]

39. Heese K, Fiebich BL, Bauer J, Otten U. Nerve growth factor (NGF) expression in rat microglia is induced by adenosine A2a-receptors. Neurosci Lett. 1997; 231:83–86. [PubMed: 9291146]

40. Küst BM, Biber K, van Calker D, Gebicke-Haerter PJ. Regulation of K+ channel mRNA expression by stimulation of adenosine A2a-receptors in cultured rat microglia. Glia. 1999; 25:120–130. [PubMed: 9890627]

41. Klegeris A, Bissonnette CJ, McGeer PL. Modulation of human microglia and THP-1 cell toxicity by cytokines endogenous to the nervous system. Neurobiol Aging. 2005; 26:673–682. [PubMed: 15708442]

42. Bystrova MF, Yatzenko YE, Fedorov IV, Rogachevskaja OA, Kolesnikov SS. P2Y isoforms operative inmouse taste cells. Cell Tissue Res. 2006; 323:377–382. [PubMed: 16328495]

43. Bianco F, et al. Pathophysiological roles of extracellular nucleotides in glial cells: differential expression of purinergic receptors in resting and activated microglia. Brain Res Brain Res Rev. 2005; 48:144–156. [PubMed: 15850653]

44. Hoskin DW, Butler JJ, Drapeau D, Haeryfar SM, Blay J. Adenosine acts through an A3 receptor to prevent the induction of murine anti-CD3-activated killer T cells. Int J Cancer. 2002; 99:386–395. [PubMed: 11992407]

45. Grijelmo C, et al. Proinvasive activity of BMP-7 through SMAD4/src-independent and ERK/Rac/JNK-dependent signaling pathways in colon cancer cells. Cell Signal. 2007; 19:1722–1732. [PubMed: 17478078]

46. Chen Y, Shukla A, Namiki S, Insel PA, Junger WG. A putative osmoreceptor system that controls neutrophil function through the release of ATP, its conversion to adenosine, and activation of A2 adenosine and P2 receptors. J Leukocyte Biol. 2004; 76:245–253. [PubMed: 15107462]

47. Feng C, Mery AG, Beller EM, Favot C, Boyce JA. Adenine nucleotides inhibit cytokine generation by human mast cells through a Gs-coupled receptor. J Immunol. 2004; 173:7539–7547. [PubMed: 15585881]

48. Kyrkanides S, et al. Cyclooxygenase-2 modulates brain inflammation-related gene expression in central nervous system radiation injury. Brain Res Mol Brain Res. 2002; 104:159–169. [PubMed: 12225870]

49. Tha KK, et al. Changes in expression of proinflammatory cytokines IL-1beta, TNF-alpha and IL-6 in the brain of senescence accelerated mouse (SAM) P8. Brain Res. 2000; 885:25–31. [PubMed: 11121526]

50. Park JS, Woo MS, Kim SY, Kim WK, Kim HS. Repression of interferon-gamma-induced inducible nitric oxide synthase (iNOS) gene expression in microglia by sodium butyrate is mediated through specific inhibition of ERK signaling pathways. J Neuroimmunol. 2005; 168:56–64. [PubMed: 16091294]
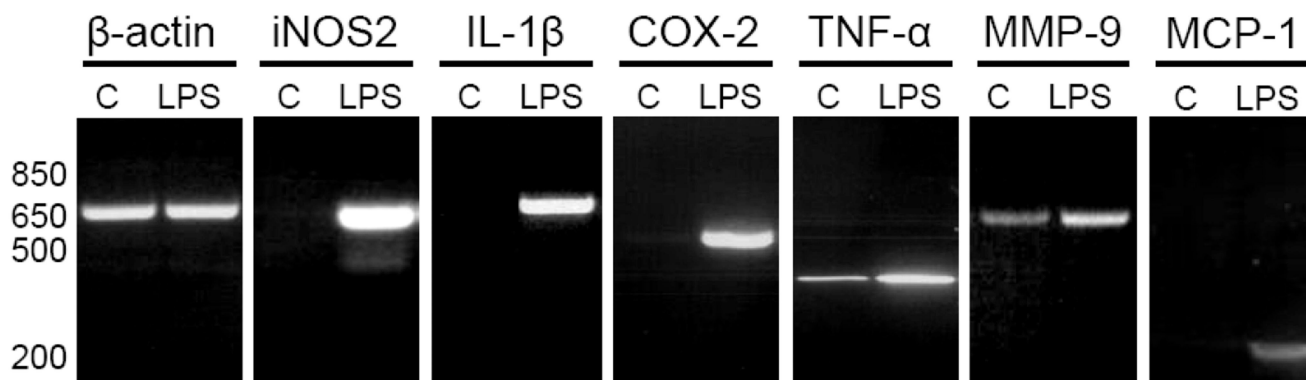
Fig. 1. Untreated microglia exhibit low expression of activation markers
RT-PCR analysis in cultured mouse microglia indicates that control microglia (C) exhibit low mRNA levels for known proinflammatory factors, as indicated. Upon LPS treatment (100 ng/ml, 24 h), microglia show robust upregulation of these factors (n = 3). Abbreviations: iNOS: inducible nitric oxide synthase, IL-1β interleukin-1β, COX-2: cyclooxygenase-2, TNF-α: tumor necrosis factor-α, MMP-9: matrix metalloproteinase-9, MCP-1: monocyte chemoattractant protein-1.
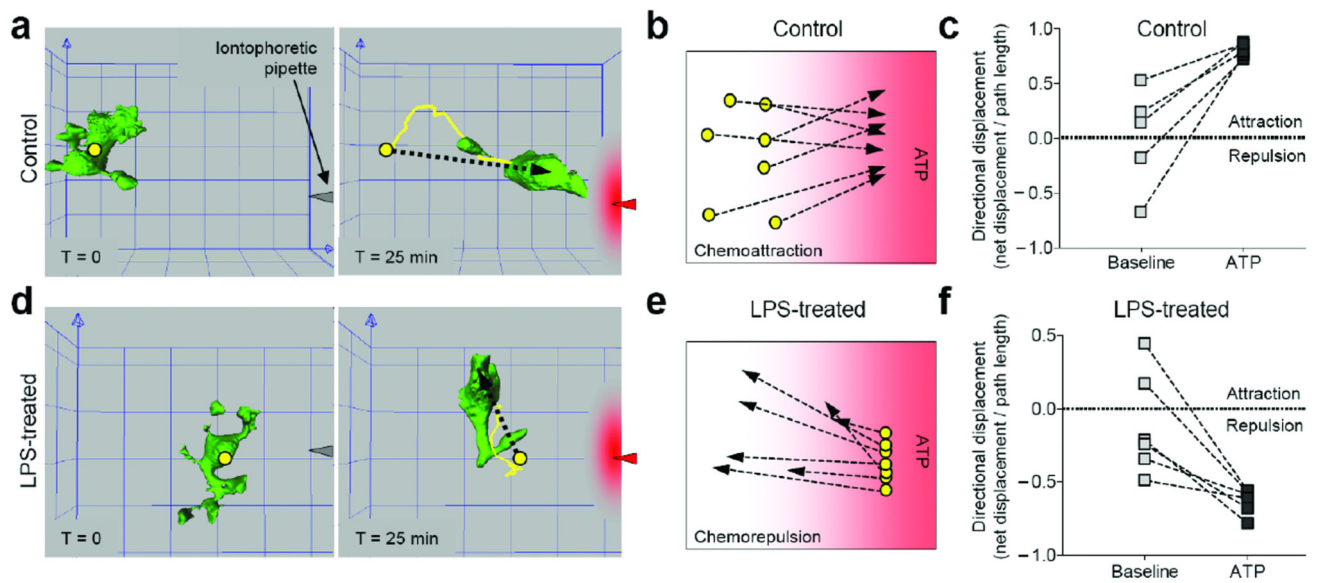
Fig. 2. ATP induces migratory repulsion in activated microglia
(**a**) Three-dimensional reconstruction of a microglial cell shown before and after 25 minutes of local ATP exposure (0.5 mM, yellow dot marks starting position of cell nucleus, yellow line shows migratory path, dashed arrow indicates net displacement of cell nucleus). Scale: 10 μm^2 per grid square. (**b**) Vector displacement of microglia during ATP ejection for 1 hour, as plotted after X-axis alignment to pipette tip location. (**c**) Microglia exhibit enhanced migration toward ATP source (n = 5, p < 0.05 compared to baseline). Negative values were assigned for net migration away from pipette. (**d**–**f**) LPS-activated microglia migrate away from ATP (LPS: 100 ng/ml; n = 6, p < 0.01 compared to baseline).
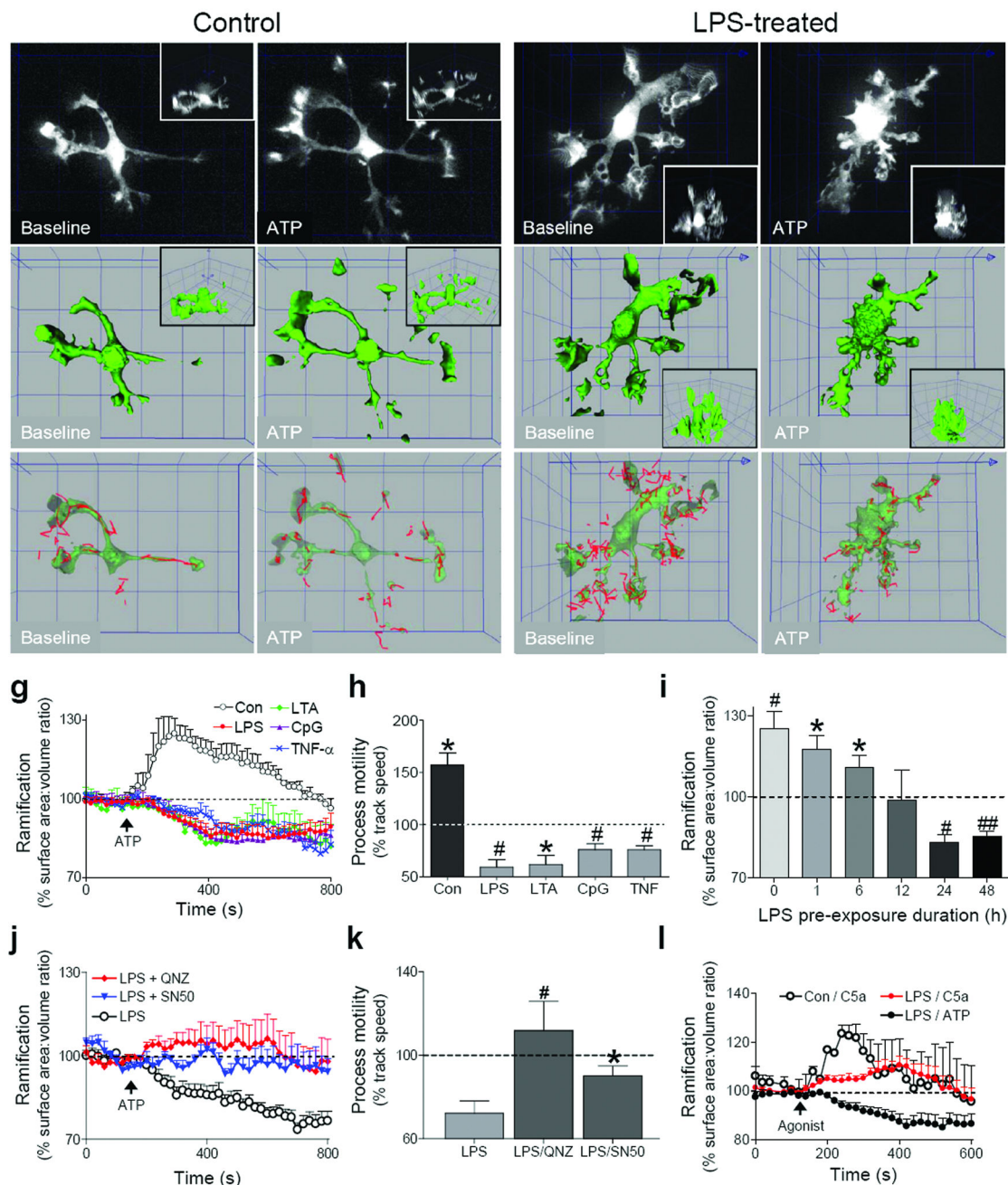
Fig. 3. ATP induces process retraction and slowed motility in activated microglia
Microglial three-dimensional volume (**a**, **b**), surface (**c**, **d**), and tracked process movement (**e**, **f**) during baseline and ATP exposure (Scale: 10 μm² per grid square). (**g**) ATP increases process ramification in control microglia (Con, n = 6, p < 0.01 compared to baseline), but causes retraction in activated microglia (n = 5–10; LPS: p < 0.01; LTA: 10 μg/ml, p < 0.01; CpG: 10 μM, p < 0.001; TNF-α: 20 ng/ml, p < 0.001; compared to baseline). (**h**) ATP increases motility in control microglia, but decreases motility in activated microglia (n = 6–8, compared to baseline, pre-ATP baseline was set to 100% track speed). (**i**) Chemotactic

reversal requires > 12 hours (n = 4–8, compared to baseline). (**j**) Process retraction is blocked by NF-κB inhibitors (1 μM QNZ, 20 μM SN50, n = 6–10, p < 0.05 compared to responses in LPS-activated cells). (**k**) NF-κB inhibition prevents ATP-induced decline in process motility (n = 4–5, compared to responses in LPS-activated cells; pre-ATP baseline was set to 100% track speed). (**l**) C5a (20 nM) increases ramification in LPS-activated microglia (n = 8, p < 0.05 compared to baseline). All graphs show mean + s.e.m; *p < 0.05, #p < 0.01, ##p < 0.001
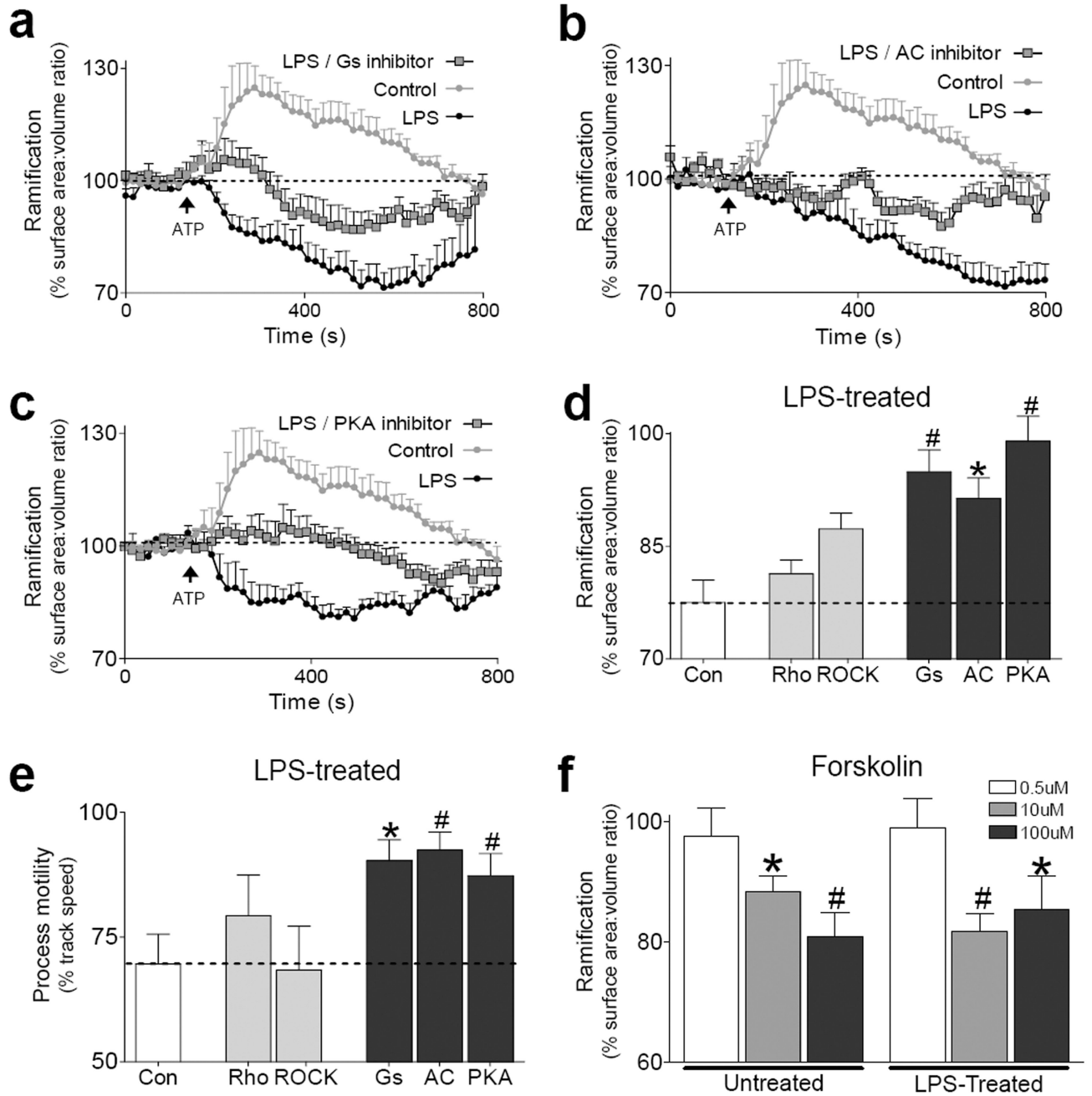
Fig. 4. Gs-coupled signaling mediates microglial repulsion from ATP

(a–c) Microglial process retraction was attenuated by inhibition of $G\alpha_s$ with NF449 (50 μM, n = 8), inhibition of adenylate cyclase (AC) with ddAdo (50 μM, n = 6), or inhibition of PKA with H89 (50 μM, n = 8). (d) Summary of inhibitor effects on retraction in LPS-activated microglia (Con) is shown. Inhibition of Rho with C3 exoenzyme (20 μg/ml, n = 5) or ROCK with Y27632 (10 μM, n = 9) had no effect. (e) Process motility decline in activated microglia was attenuated with $G\alpha_s$, AC, or PKA inhibitors, but not with Rho or ROCK inhibitors. For graphs a–e: values were compared to responses in LPS-treated cells.

(**f**) Adenylate cyclase activation with forskolin triggered retraction in both control and activated microglia (values were compared to baseline). All graphs show mean + s.e.m. *p < 0.05, #p < 0.01, ##p < 0.001.
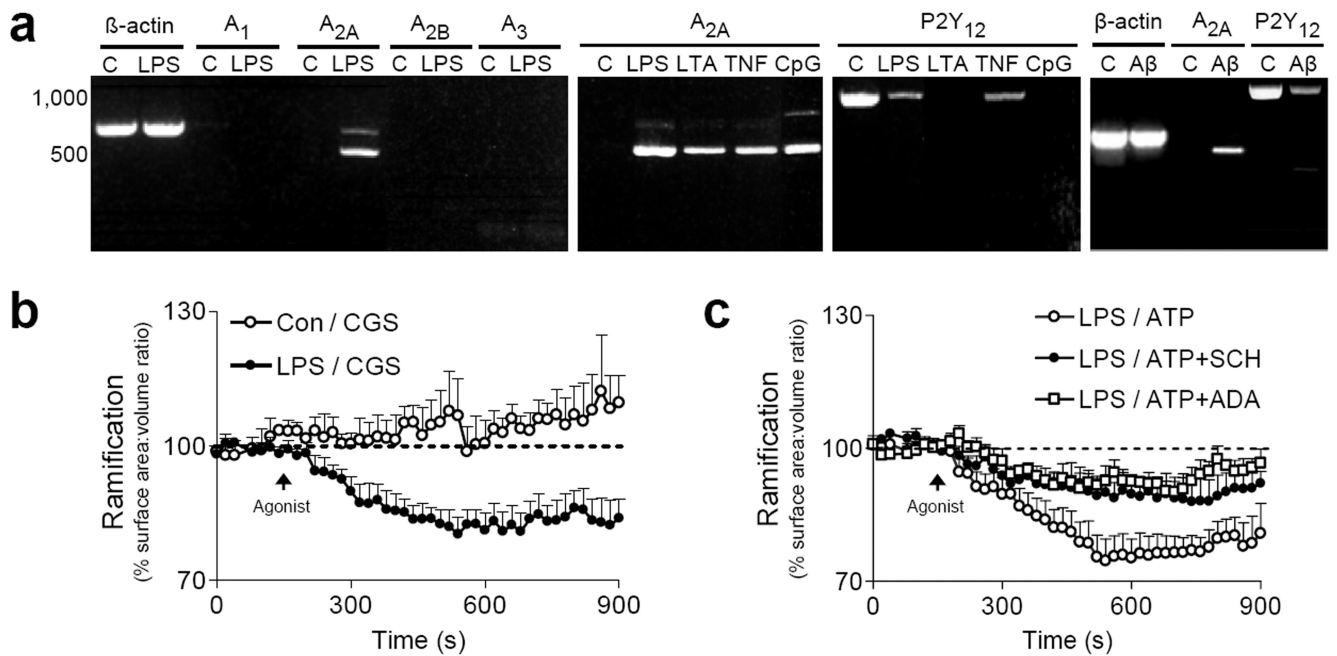
Fig. 5. Adenosine A$_{2A}$ receptor upregulation mediates process retraction and reverses chemotaxis in activated microglia

(**a**) A$_{2A}$ receptor mRNA is upregulated upon microglial activation with LPS (n = 4), LTA (n = 3), TNF-α (n = 3), CpG (n = 2), or amyloid-β (Aβ, n = 3, 1 μM), while P2Y$_{12}$ is downregulated. (**b**) A$_{2A}$ agonist triggered retraction in LPS-treated microglia (CGS: 20 μM, n = 6, p < 0.01 compared to baseline), but not in untreated cells (Con: n = 3). (**c**) The A$_{2A}$ antagonist SCH-58261 (SCH: 5 μM) and adenosine deaminase (ADA: 5 U/ml) inhibited ATP-induced retraction in LPS-activated microglia (ATP: n = 5; ATP + SCH: n = 7, p < 0.05; ATP + ADA: n = 5, p < 0.05 compared to responses in ATP-treated cells). All graphs show mean + s.e.m.
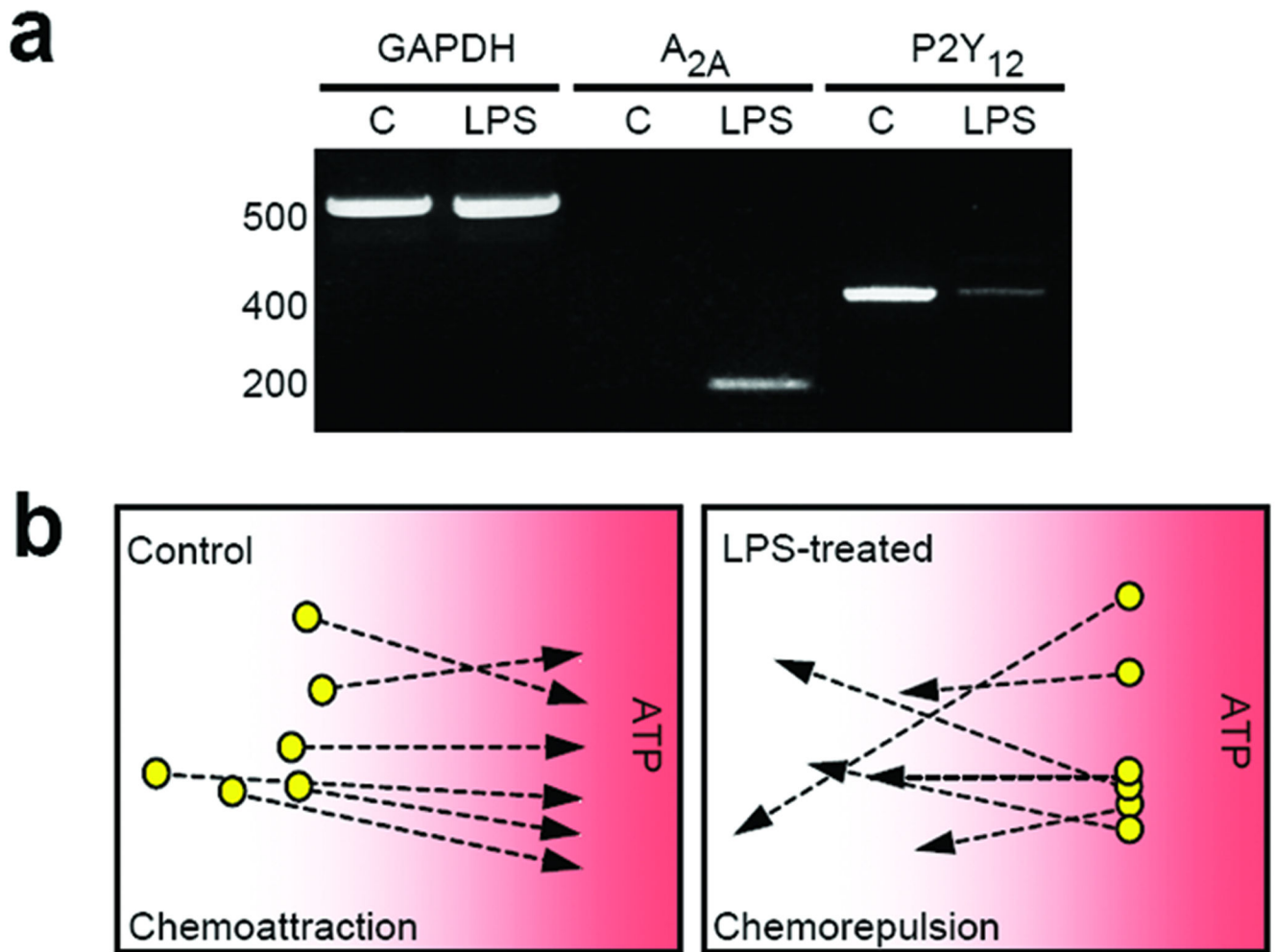
Fig. 6. Human microglia exhibit a similar shift in purinergic receptor expression and chemotactic response to ATP

(**a**) Activated human microglia upregulate A_{2A} mRNA and downregulate $P2Y_{12}$ mRNA (n = 4). (**b**) Untreated human microglia migrate toward ATP (Control: n = 6, 0.5 mM), while LPS-activated microglia migrate away from ATP (LPS: n = 5).
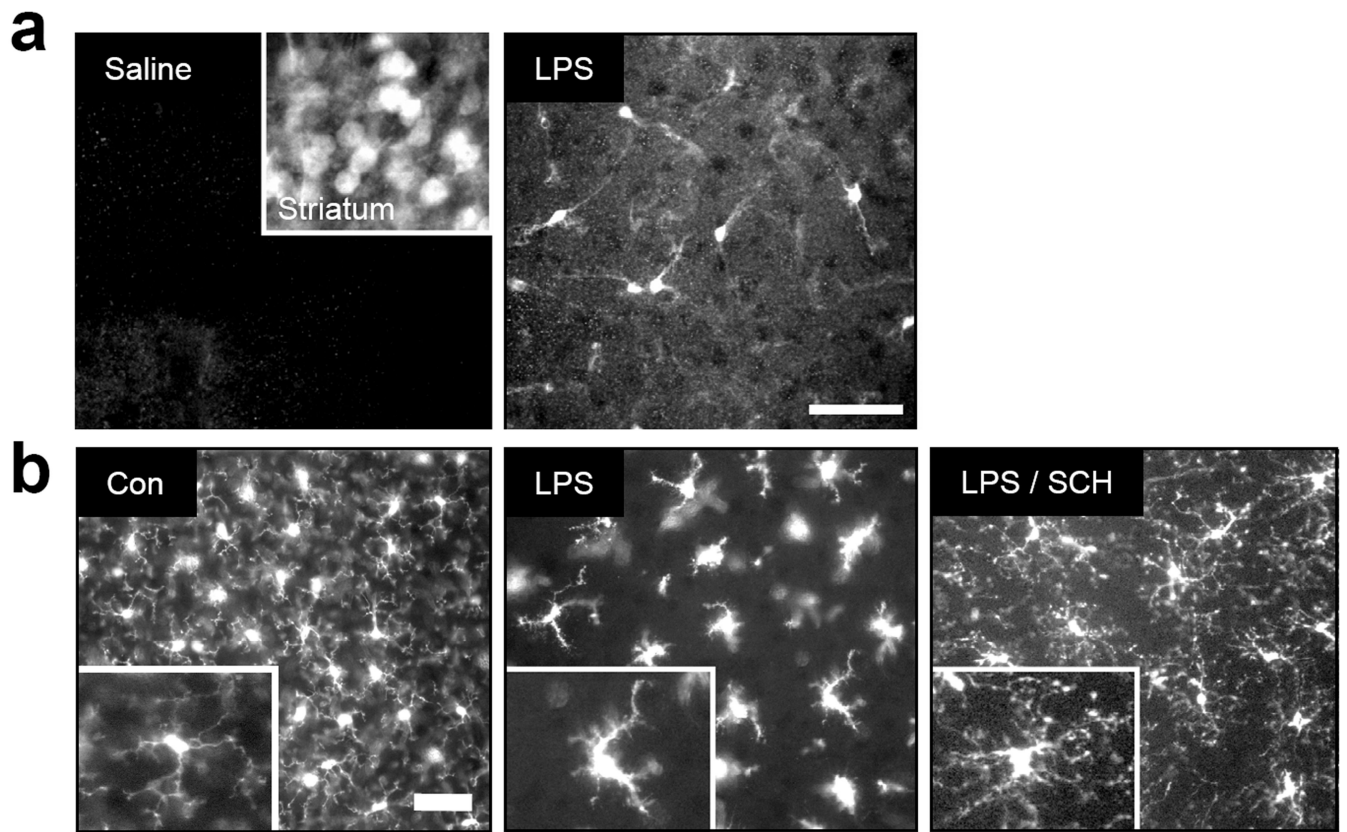
Fig. 7. A$_{2A}$ receptor upregulation and involvement in microglial retraction *in vivo*
(**a**) Fixed cortical tissue sections from BAC-transgenic mice expressing eGFP upstream of
BAC A$_{2A}$ coding sequence were immunostained for eGFP. LPS-treated animals (LPS: 2
mg/kg) exhibit A$_{2A}$ upregulation after 48 hours, as evidenced by increased eGFP expression.
Scale bar: 50 μm. *Inset*: Constitutive A$_{2A}$ expression within striatal neurons served as a
positive control. (**b**) Fixed cortical tissue sections from *Cx3cr1-eGFP* transgenic mice.
Intracortical blockade of the A$_{2A}$ receptor with the antagonist SCH-58261 (SCH: 1 mM)
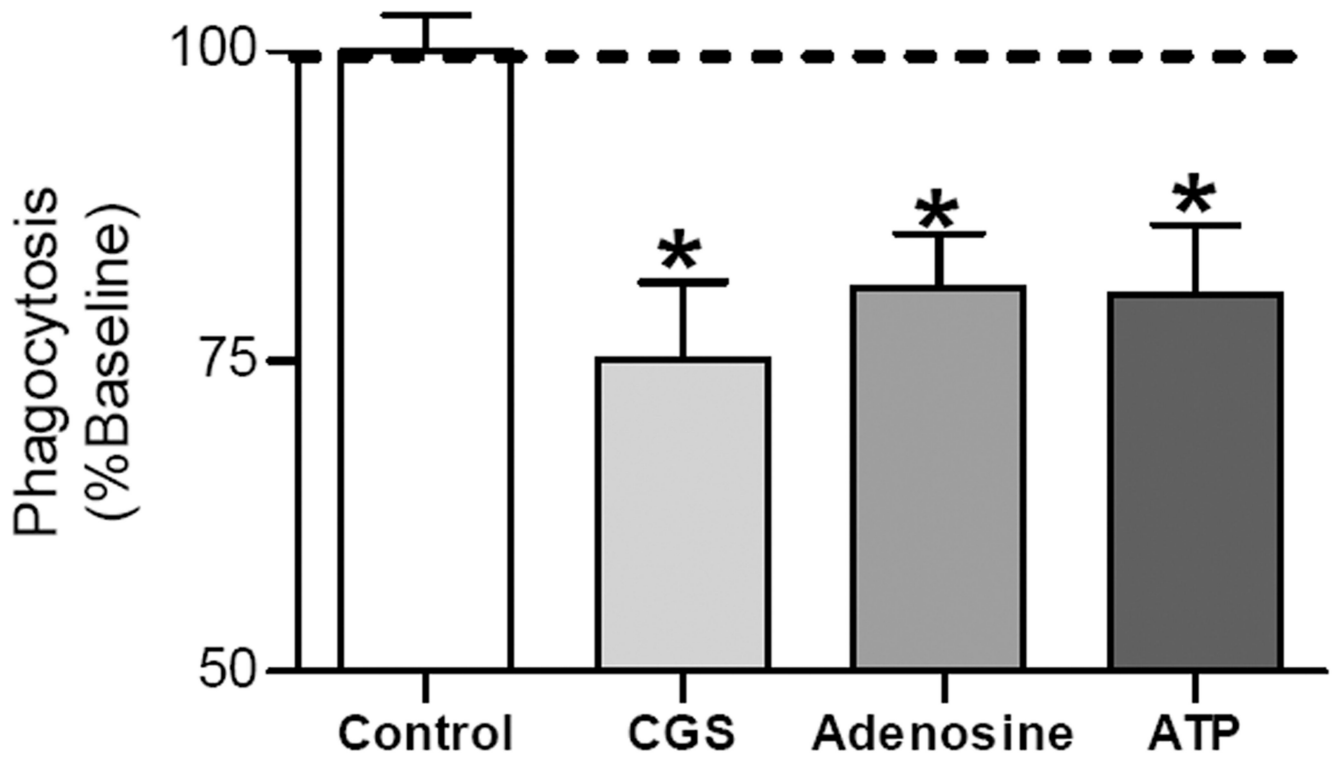triggered microglial process ramification in LPS-exposed animals (n = 4; scale bar: 50 μm).

Fig. 8. A$_{2A}$ stimulation inhibits uptake by LPS-treated microglia
Treatment with indicated agonists (50 μM) for 20 minutes following microglial exposure to LPS (100 ng/ml, 24 h) led to a decline in microglial uptake of fluorescein-labeled *E. coli* bioparticles, which were applied for 2 hours along with agonists. CGS-21680 (CGS). n ≥ 7, *p < 0.05. Graph shows mean + s.e.m.